Appl. Math. Mech. -Engl. Ed., **42**(12), 1733–1742 (2021)

APPLIED MATHEMATICS AND MECHANICS (ENGLISH EDITION)

https://doi.org/10.1007/s10483-021-2799-7

Low-velocity impact of rectangular foam-filled fiber metal laminate tubes*

Jianxun ZHANG[1,2,†], Haoyuan GUO[1]

1. State Key Laboratory for Strength and Vibration of Mechanical Structures, School of Aerospace Engineering, Xi'an Jiaotong University, Xi'an 710049, China;
2. Jiangsu Key Laboratory of Engineering Mechanics, Southeast University, Nanjing 211189, China

(Received Jun. 15, 2021 / Revised Oct. 8, 2021)

Abstract Through theoretical analysis and finite element simulation, the low-velocity impact of rectangular foam-filled fiber metal laminate (FML) tubes is studied in this paper. According to the rigid-plastic material approximation with modifications, simple analytical solutions are obtained for the dynamic response of rectangular foam-filled FML tubes. The numerical calculations for low-velocity impact of rectangular foam-filled FML tubes are conducted. The accuracy of analytical solutions and numerical results is verified by each other. Finally, the effects of the metal volume fraction of FMLs, the number of the metal layers in FMLs, and the foam strength on the dynamic response of foam-filled tubes are discussed through the analytical model in details. It is shown that the force increases with the increase in the metal volume fraction in FMLs, the number of the metal layers in FML, and the foam strength for the given deflection.

Key words fiber metal laminate (FML) tube, metal foam, low-velocity impact, energy absorption

Chinese Library Classification O317
2010 Mathematics Subject Classification 70K20

1 Introduction

The fiber metal laminate (FML) is composed of thin aluminum alloy sheets and fiber reinforced epoxy adhesive layers alternately. This combination combines the advantages of com-

* Citation: ZHANG, J. X. and GUO, H. Y. Low-velocity impact of rectangular foam-filled fiber metal laminate tubes. *Applied Mathematics and Mechanics* (*English Edition*), **42**(12), 1733–1742 (2021) https://doi.org/10.1007/s10483-021-2799-7

† Corresponding author, E-mail: jianxunzhang@mail.xjtu.edu.cn

Project supported by the National Natural Science Foundation of China (Nos. 11872291 and 11972281), the Jiangsu Key Laboratory of Engineering Mechanics, Southeast University, the Fundamental Research Funds for the Central Universities (No. LEM21B01), the Key Laboratory of Impact and Safety Engineering (Ningbo University), Ministry of Education (No. cj202002), and the Natural Science Basic Research Plan in Shaanxi Province of China (No. 2020JM-034)

posites and metals while avoids their respective disadvantages. The FML has the advantages of lightweight, good fatigue properties, high damage tolerance, corrosion resistance, and fire resistance[1–2], and it has become a very attractive material in aerospace, automobile, and ship fields. Metal foam[3–10] is a kind of lightweight material with lightweight, high specific strength and high specific stiffness. Metal foam is filled in the FML tube, and combined into the foam-filled FML tube. This structure can be widely used in aerospace, ship traffic, vehicle safety and other fields.

Some scholars have studied the static and dynamic characteristics of foam-filled tubes. Hall et al.[11] carried out lateral compressive tests of aluminum, brass, and titanium tubes filled with and without aluminum foam. Niknejad et al.[12] studied the effect of polyurethane foam filler on the transverse plastic deformation of the metal tube under a radial quasi-static loading. It is found that the polyurethane foam filler improves energy absorption of the metal tube, the increment of energy absorption of the thin metal tube is bigger than that of the thick metal tube. Niknejad et al.[13] conducted the compressive tests on the E-glass/vinylester composite tubes filled with and without polyurethane foam. The results show that increasing the length of composite tube and the number of fiber layers can enhance the energy absorption under a transverse compression. Fang et al.[14] studied the dynamic response and optimization of functionally gradient foam filled square tubes under transverse impact by experiments and finite element simulation. Niknejad and Rahmani[15] studied the response of polyurethane foam-filled hexagon tube under the quasi-static transverse loading by theoretical and experimental methods. Yan et al.[16] carried out quasi-static compressive tests of the polyurethane foam-filled natural flax fiber reinforced epoxy composite tube. The experimental results show that the use of polyurethane foam inhibits fiber fracture and ultimately increases the energy absorption of composite tube during transverse compression. Elahi et al.[17] analytically studied the energy absorption characteristics of the polyurethane foam-filled woven fabric circular tube during transverse loading between rigid plates. Su et al.[18] studied the transverse compressive characteristics of alumina-aluminum foam filled tubes by the experimental method. It is found that the energy absorption of the foam-filled tube is higher than the sum of the components. Zhang et al.[19] conducted the quasi-static lateral compressive test of cenosphere/aluminum syntactic circular foam-filled tubes, and numerically studied mechanical properties and energy absorption properties of the foam-filled tubes. Zhu et al.[20] experimentally studied the energy absorption and crashworthiness of laterally crushed thin-walled structures filled with aluminum foam and carbon fibre reinforced plastics skeleton. An et al.[21] studied the dynamic response of square foam-filled tube with functional lateral graded thickness (FLGT) sheets under transverse impact loading by means of experiments and finite element simulation. The numerical results show that the FLGT structure has obvious advantages in specific energy absorption compared with the uniform thickness structure under transverse loading for the same weight.

There are few studies on the dynamic response of FML tubes. Shiravand and Asgari[22] presented a theoretical solution for FML conical tubes with arbitrary number of metal and composite layers, and verified the average limit load based on the theoretical solution by experiments and finite element calculation. Mansor et al.[23] studied the energy absorption and impact characteristics of seamless FML tubes through axial low-velocity impact experiments.

The analytical investigations on dynamic response of foam-filled FML tubes were few. The purpose of the present work is to study the low-velocity impact of rectangular foam-filled FML tubes. In Section 2, the problem description is presented. In Section 3, the analytical force-deflection and initial impact energy-maximum deflection relations for low-velocity impact of

rectangular foam-filled FML tubes are given. In Section 4, the finite element simulation is carried out. In Section 5, the analytical results are compared with finite element ones. Then, based on the theoretical model, the effects of metal volume fraction in FMLs, the number of the metal layers in FMLs, and the foam strength on dynamic response of the foam-filled tubes are discussed. In Section 6, conclusions are presented.

2 Problem description

Consider a clamped rectangular foam-filled FML tube with wide b, high b_1, span $2L$, thickness of tube-wall h, and mass per unit length G_t. The foam-filled tube is struck by a striker with low-velocity impact of V_I and heavy mass of G in Fig. 1. Suppose that the metal foam is perfectly filled and bonded to the tube. It is assumed the metal layer in foam-filled FML tube follows rigid-perfectly plastic rule with yield stress σ_m. The tensile strength of the composite layer in FML is σ_f. The filled metal foam obeys rigid-perfectly plastic locking model with platform stress σ_c and densification strain ε_D.

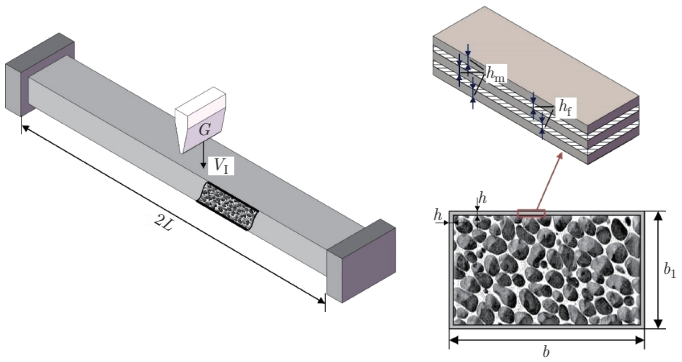

Fig. 1 Schematic diagram of rectangular foam-filled FML tube under low-velocity impact (color online)

It is assumed that the FML consists of n metal layers with thickness of h_m and $n-1$ composite layers with thickness of h_f. Thus,

$$h = nh_\mathrm{m} + (n-1)h_\mathrm{f}. \tag{1}$$

3 Analytical model

If the plastic behavior plays an important role in the deformation for the FML structure, the theoretical rigid plastic solution can be used to predict dynamic characteristics of the FML structure under low-velocity impact[24]. This method is extended to analyze the dynamic response of rectangular foam-filled FML tubes under low-velocity impact.

The analytical solution for the dynamic response of the slender rectangular metal foam-filled tube under low-velocity impact is presented as follow[25]. For the sake of completeness, the analytical solutions for dynamic response of the slender rectangular metal foam-filled tube under low-velocity impact are briefly presented here. The clamped slender rectangular foam-filled tube is struck by a striker under low-velocity impact with V_I and heavy mass G. The length, width, and height of tube are $2L$, b, and b_1. It is assumed the metal foam is perfectly filled and combined in the tube with thickness h and h_1 in height and width directions. The metal tube is assumed to obey the rigid-perfectly plastic law with yield stress σ_f. The filled

metal foam obeys the rigid-perfectly plastic locking model with platform stress $\sigma_{\rm c}$, densification strain $\varepsilon_{\rm D}$. The striker is assumed to be a rigid body.

It is assumed that there is no local denting and overall bending of the slender rectangular metal foam-filled tube occurs. The cross-section shape is consistent with the initial state, and the overall bending deformation is the same as that of the solid beam under low-velocity impact. The deformation diagram of the foam-filled tube is shown in Fig. 2. The equilibrium equation of the mass-beam system at mid-span can be expressed as

$$\Big(\frac{(2\sigma_{\rm f}(bh_1+b_1h-2hh_1)+\rho_{\rm c}(b-2h)(b-2h_1))L^2}{3}+\frac{GL}{2}\Big)\ddot{W}_0+NW_0+2M=0, \tag{2}$$

where M and N are the plastic moment and axial force of the foam-filled tube, F ($\cong N$) is the horizontal force for the moderate deflection, P is the external force at impact location, and W_0 is the displacement at mid-span.

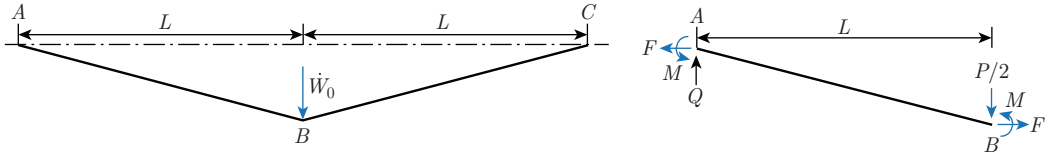

(a) Transverse deflection profile (b) Forces and moments

Fig. 2 Overall bending deformation pattern for plastic neutral surface of clamped rectangular foam-filled FML tube under low-velocity impact (color online)

The force-displacement relation of the rectangular metal foam-filled tube under low-velocity impact is[25]

$$P_{\rm r}^*=\begin{cases}\dfrac{3G^*}{3G^*+1}\Big(\dfrac{\overline{\sigma}_{\rm c}}{4(\overline{\sigma}_{\rm c}(1/2-\overline{h}_1)^2+\overline{h}_1(1-\overline{h}_1))}W_0^{*2}+1\Big), & 0\leqslant W_0^*<1-2\overline{h}_1,\\ \dfrac{3G^*}{3G^*+1}\dfrac{W_0^{*2}+2(\overline{\sigma}_{\rm c}-1)(1-2\overline{h}_1)W_0^*+1}{4(\overline{\sigma}_{\rm c}(1/2-\overline{h}_1)^2+\overline{h}_1(1-\overline{h}_1))}, & 1-2\overline{h}_1\leqslant W_0^*<1,\\ \dfrac{3G^*}{3G^*+1}\dfrac{2\overline{h}_1+\overline{\sigma}_{\rm c}(1-2\overline{h}_1)}{2(\overline{\sigma}_{\rm c}(1/2-\overline{h}_1)^2+\overline{h}_1(1-\overline{h}_1))}W_0^*, & W_0^*\geqslant 1,\end{cases} \tag{3}$$

where

$$P_{\rm r}^*=\frac{P_{\rm r}}{P_{\rm c}},\quad P_{\rm c}=\frac{4M_{\rm p}}{L},\quad M_{\rm p}=\sigma_{\rm f}bh(b_1-h)+\sigma_{\rm cf}b\Big(\frac{1}{2}b_1-h\Big)^2,\quad \sigma_{\rm cf}=\sigma_{\rm m}\frac{2h}{b}+\sigma_{\rm c}\frac{b-2h}{b},$$

$$\overline{\sigma}_{\rm c}=\frac{\sigma_{\rm cf}}{\sigma_{\rm f}}=2\overline{h}+\overline{\sigma}(1-2\overline{h}),\quad \overline{\sigma}=\frac{\sigma_{\rm c}}{\sigma_{\rm m}},\quad \overline{h}=\frac{h}{b},\quad \overline{h}_1=\frac{h}{b_1},\quad W_0^*=\frac{W_0}{b_1},\quad G^*=\frac{G}{2G_{\rm t}L}.$$

The initial impact energy-maximum deflection relation of the rectangular metal foam-filled tube under low-velocity impact is[25]

$$\frac{4G^*(1+3G^*)}{3(1+2G^*)^2}U_{\rm K}^*=\begin{cases}\dfrac{\overline{\sigma}_{\rm c}}{12(\overline{\sigma}_{\rm c}(1/2-\overline{h}_1)^2+\overline{h}_1(1-\overline{h}_1))}W_{0\rm m}^{*3}+W_{0\rm m}^*, & 0\leqslant W_{0\rm m}^*<1-2\overline{h},\\ \dfrac{W_{0\rm m}^{*3}+3(\overline{\sigma}_{\rm c}-1)(1-2\overline{h}_1)W_{0\rm m}^{*2}+3W_{0\rm m}^*}{12(\overline{\sigma}_{\rm c}(1/2-\overline{h}_1)^2+\overline{h}_1(1-\overline{h}_1))}+K_1, & 1-2\overline{h}_1\leqslant W_{0\rm m}^*<1,\\ \dfrac{2\overline{h}_1+\overline{\sigma}_{\rm c}(1-2\overline{h}_1)}{4(\overline{\sigma}_{\rm c}(1/2-\overline{h}_1)^2+\overline{h}_1(1-\overline{h}_1))}W_{0\rm m}^{*2}+K_2, & W_{0\rm m}^*\geqslant 1,\end{cases} \tag{4}$$

where

$$U_{\mathrm{K}}^{*}=\frac{GV_{\mathrm{I}}^{2}}{2P_{\mathrm{c}}b_{1}},\quad K_{1}=\frac{(\overline{\sigma}_{\mathrm{c}}-1)(1-2\overline{h}_{1})^{3}}{12(\overline{\sigma}_{\mathrm{c}}(1/2-\overline{h}_{1})^{2}+\overline{h}_{1}(1-\overline{h}_{1}))},\quad K_{2}=\frac{(\overline{\sigma}_{\mathrm{c}}-1)(1-2\overline{h}_{1})^{3}+1}{12(\overline{\sigma}_{\mathrm{c}}(1/2-\overline{h}_{1})^{2}+\overline{h}_{1}(1-\overline{h}_{1}))}.$$

The volume fraction of metal layers in FMLs is defined as[24]

$$f=\frac{nh_{\mathrm{m}}}{h}\times 100\%. \tag{5}$$

The average strength of FML is defined as[24]

$$\sigma_{\mathrm{fa}}=f\sigma_{\mathrm{m}}+(1-f)\sigma_{\mathrm{f}}. \tag{6}$$

Substituting Eqs. (1), (5), and (6) into Eqs. (3) and (4), the analytical solutions of the dynamic response of the rectangular foam-filled FML tube under low-velocity impact can be obtained. The force-deflection formula of the rectangular foam-filled FML tube under low-velocity impact is given by

$$P_{\mathrm{r}}^{*}=\begin{cases}\dfrac{3G^{*}}{3G^{*}+1}\Big(\dfrac{\overline{\sigma}_{\mathrm{c}}(1-f)^{2}}{\overline{\sigma}_{\mathrm{c}}(1-f-2\overline{h}_{\mathrm{f}}(n-1))^{2}+4\overline{h}_{\mathrm{f}}(n-1)(1-f-\overline{h}_{\mathrm{f}}(n-1))}W_{0}^{*2}+1\Big),\\ 0\leqslant W_{0}^{*}<1-\dfrac{2\overline{h}_{\mathrm{f}}(n-1)}{1-f},\\ \dfrac{3G^{*}}{3G^{*}+1}\dfrac{(1-f)((1-f)W_{0}^{*2}+2(\overline{\sigma}_{\mathrm{c}}-1)(1-f-2\overline{h}_{\mathrm{f}}(n-1))W_{0}^{*}+1-f)}{\overline{\sigma}_{\mathrm{c}}(1-f-2\overline{h}_{\mathrm{f}}(n-1))^{2}+4\overline{h}_{\mathrm{f}}(n-1)(1-f-\overline{h}_{\mathrm{f}}(n-1))},\\ 1-\dfrac{2\overline{h}_{\mathrm{f}}(n-1)}{1-f}\leqslant W_{0}^{*}<1,\\ \dfrac{3G^{*}}{3G^{*}+1}\dfrac{2(1-f)(2\overline{h}_{\mathrm{f}}(n-1)(1-2\overline{\sigma}_{\mathrm{c}})+\overline{\sigma}_{\mathrm{c}}(1-f))}{\overline{\sigma}_{\mathrm{c}}(1-f-2\overline{h}_{\mathrm{f}}(n-1))^{2}+4\overline{h}_{\mathrm{f}}(n-1)(1-f-\overline{h}_{\mathrm{f}}(n-1))}W_{0}^{*},\quad W_{0}^{*}\geqslant 1,\end{cases} \tag{7}$$

where

$$\overline{h}_{\mathrm{f}}=\frac{h_{\mathrm{f}}}{b_{1}},\quad \overline{\sigma}_{\mathrm{c}}=\frac{\sigma_{\mathrm{cf}}}{\sigma_{\mathrm{f}}}=2\overline{h}(1+f(q-1))+\overline{\sigma}_{1}(1-2\overline{h}),$$
$$\sigma_{\mathrm{cf}}=2\overline{h}\sigma_{\mathrm{fa}}+(1-2\overline{h})\sigma_{\mathrm{c}},\quad q=\frac{\sigma_{\mathrm{m}}}{\sigma_{\mathrm{f}}},\quad \overline{\sigma}_{1}=\frac{\sigma_{\mathrm{c}}}{\sigma_{\mathrm{f}}},\quad \overline{h}=\frac{h}{b}=\frac{n-1}{1-f}\frac{h_{\mathrm{f}}}{b},$$
$$\sigma_{\mathrm{fa}}=f\sigma_{\mathrm{m}}+(1-f)\sigma_{\mathrm{f}},\quad M_{\mathrm{p}}=\sigma_{\mathrm{fa}}bh(b_{1}-h)+\sigma_{\mathrm{cf}}b(b_{1}/2-h)^{2}.$$

The initial impact energy-maximum deflection relation of the rectangular foam-filled FML tube under low-velocity impact is

$$\frac{4G^{*}(1+3G^{*})}{3(1+2G^{*})^{2}}U_{\mathrm{K}}^{*}$$
$$=\begin{cases}\dfrac{\overline{\sigma}_{\mathrm{c}}(1-f)^{2}}{3\overline{\sigma}_{\mathrm{c}}(1-f-2\overline{h}_{\mathrm{f}}(n-1))^{2}+4\overline{h}_{\mathrm{f}}(n-1)(1-f-\overline{h}_{\mathrm{f}}(n-1))}W_{0\mathrm{m}}^{*3}+W_{0\mathrm{m}}^{*},\\ 0\leqslant W_{0\mathrm{m}}^{*}<1-\dfrac{2\overline{h}_{\mathrm{f}}(n-1)}{1-f},\\ \dfrac{(1-f)((1-f)W_{0\mathrm{m}}^{*3}+3(\overline{\sigma}_{\mathrm{c}}-1)(1-f-2h_{\mathrm{f}}(n-1))(1-2\overline{h}_{1})W_{0\mathrm{m}}^{*2}+(1-f)3W_{0\mathrm{m}}^{*})}{3\overline{\sigma}_{\mathrm{c}}(1-f-2\overline{h}_{\mathrm{f}}(n-1))^{2}+4\overline{h}_{\mathrm{f}}(n-1)(1-f-\overline{h}_{\mathrm{f}}(n-1))}\\ +K_{3},\quad 1-\dfrac{2\overline{h}_{\mathrm{f}}(n-1)}{1-f}\leqslant W_{0\mathrm{m}}^{*}<1,\\ \dfrac{(1-f)(2\overline{h}_{\mathrm{f}}(n-1)(1-2\overline{\sigma}_{\mathrm{c}})+\overline{\sigma}_{\mathrm{c}}(1-f))}{\overline{\sigma}_{\mathrm{c}}(1-f-2\overline{h}_{\mathrm{f}}(n-1))^{2}+4\overline{h}_{\mathrm{f}}(n-1)(1-f-\overline{h}_{\mathrm{f}}(n-1))}W_{0\mathrm{m}}^{*2}+K_{4},\quad W_{0\mathrm{m}}^{*}\geqslant 1,\end{cases} \tag{8}$$

where

$$U_{\mathrm{K}}^{*}=\frac{G_{\mathrm{t}}V_{\mathrm{I}}^{2}}{2P_{\mathrm{c}}b_{1}},\quad K_{1}=\frac{(\overline{\sigma}_{\mathrm{c}}-1)(1-f-2\overline{h}_{\mathrm{f}}(n-1))^{3}}{3(1-f)(\overline{\sigma}_{\mathrm{c}}(1-f-2\overline{h}_{\mathrm{f}}(n-1))^{2}+4\overline{h}_{\mathrm{f}}(n-1)(1-f-\overline{h}_{\mathrm{f}}(n-1)))},$$

$$K_{2}=\frac{(\overline{\sigma}_{\mathrm{c}}-1)(1-f-2\overline{h}_{\mathrm{f}}(n-1))^{3}+(1-f)^{3}}{3(1-f)(\overline{\sigma}_{\mathrm{c}}(1-f-2\overline{h}_{\mathrm{f}}(n-1))^{2}+4\overline{h}_{\mathrm{f}}(n-1)(1-f-\overline{h}_{\mathrm{f}}(n-1)))}.$$

4 Finite element (FE) analysis

FE analysis is performed to study the low-velocity impact of clamped rectangular foam-filled FML tubes using the commercial finite element software ABAQUS/explicit. Three dimensional eight-node linear brick elements (C3D8R type) with reduced integration are used to model FML tubes and metal foam. The striker is a rigid body with a predefined velocity. The check of the sensitivity of the mesh in the calculation shows that the additional mesh refinement can not change results obviously. The vertical, horizontal, and rotational displacements of the ends of rectangular foam-filled FML tubes are zero. The general contact without friction is adopted.

The half-span length of the foam-filled tube is $L = 400$ mm, the width of the tube is $b = 50$ mm, the height of tube is $b_1 = 20$ mm, the thickness of the metal layer in FML is $h_{\mathrm{m}} = 0.5$ mm, the thickness of the composite layer is $h_{\mathrm{f}} = 0.2$ mm, the number of metal layer is $n = 2$, the total thickness of FML is $h = 1.2$ mm, and the radius of the striker is $R = 4$ mm.

The metal layer of the FML tube follows the plastic flow theory. The yield strength is $\sigma_{\mathrm{m}} = 460$ MPa, elastic modulus is $E_{\mathrm{m}} = 70$ GPa, elastic Poisson's ratio is $\nu_{\mathrm{em}} = 0.3$, linear hardening modulus is $E_{\mathrm{tm}} = 0.01E_{\mathrm{m}}$ and density of the metal layer is $\rho_{\mathrm{m}} = 2\ 800\ \mathrm{kg}\cdot\mathrm{m}^{-3}$, According to the experimental data[26], the woven glass composite layer of FML includes quasi-isotropic glass fiber fabric. For the case of stretching of FML, it is assumed that the material is linear elastic[26] with tensile strength $\sigma_{\mathrm{f}} = 220$ MPa, elastic modulus $E_{\mathrm{f}} = 10$ GPa, elastic Poisson's ratio $\nu_{\mathrm{ef}} = 0.3$, and density $\rho_{\mathrm{f}} = 1\ 700\ \mathrm{kg}\cdot\mathrm{m}^{-3}$.

Deshpande-Fleck constitutive model[27] is used to model crushing characteristics of the metal foam used in ABAQUS. The yield strength of the isotropic metal foam is $\sigma_{\mathrm{c}} = 10$ MPa, elastic modulus is $E_{\mathrm{c}} = 2$ GPa, elastic Poisson's ratio is $\nu_{\mathrm{ec}} = 0.3$, plastic Poisson's ratio is $\nu_{\mathrm{p}} = 0$. The metal foam has a long platform stress σ_{c} until the densification strain reaches. After densification, the stress increases linearly with tangent modulus $E_{\mathrm{ct}} = 0.2E_{\mathrm{m}}$. FML tubes and metal foam are assumed to have enough ductility to withstand the deformation without fracture.

5 Results and discussion

Figure 3 shows the analytical and numerical results for force-deflection curves of the bottom surface of rectangular foam-filled FML tubes at mid-span subject to low-velocity impact. It can be seen that the analytical results are in good agreement with numerical ones. The neglect of elastic deformation in the analytical solution leads to the inconsistency in small deflection. Also, the analytical solution does not consider the effects of inertia effect, shear force, strain hardening of the materials. Numerical results have obvious oscillation in the initial stage, which may be caused by the complex interaction between the striker and foam-filled tube.

Figure 4 shows the analytical and numerical results for the maximum deflection curves with initial impact energy of rectangular foam-filled FML tubes under low-velocity impact. In Fig. 4(a), $G^{*} = 400$, the initial velocity is changed. In Fig. 4(b), $V_{\mathrm{I}} = 2$ m/s, the mass of the striker is variable. It can be seen from Fig. 4 that numerical results are almost slightly higher

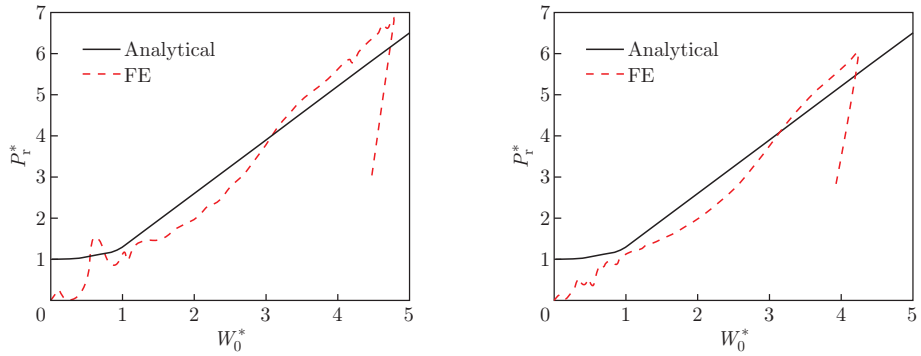

(a) $G^*=400$, $V_I=4$ m·s^{-1} (b) $G^*=1\ 200$, $V_I=2$ m·s^{-1}

Fig. 3 Analytical and numerical results for force versus deflection at impact location of foam-filled FML tubes under low-velocity impact (color online)

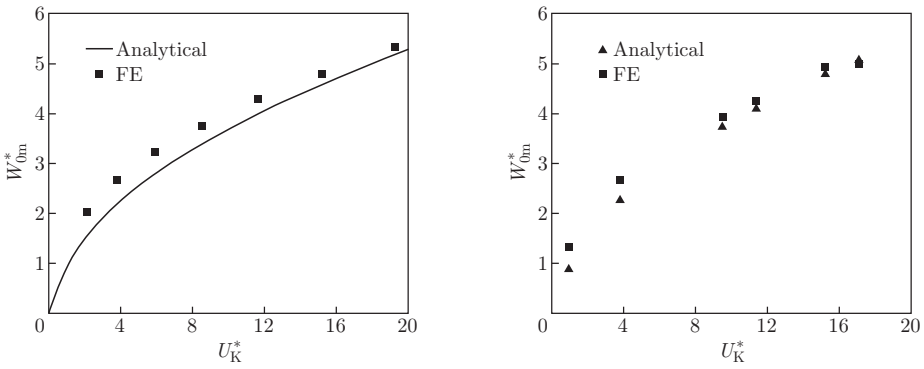

(a) $G^*=400$ (b) $V_I=2$ m·s^{-1}

Fig. 4 Analytical and numerical results for maximum deflection curves with initial impact energy of foam-filled FML tubes under low-velocity impact (color online)

than the analytical predictions, and analytical results are in good agreement with the calculated ones, especially in the high impact energy.

Figure 5 shows the effect of metal volume fraction in FML on force versus deflection curve and maximum deflection curve with initial impact energy of foam-filled FML tubes, in which $G^* = 100$, $n = 2$, $\overline{h} = 0.024$, $q = 2.1$, $\overline{\sigma}_1 = 0.045\ 5$. The force increases with the increase of metal volume fraction of FML for the given deflection in Fig. 5(a). In Fig. 5(b), the maximum deflection of the rectangular foam-filled FML tube decreases with the increase of metal volume fraction in FML for the given impact energy.

Figure 6 shows the effect of the number of metal layers in FML on the force versus deflection curve and maximum deflection curve with initial impact energy of foam-filled FML tubes, in which $G^* = 100$, $q = 2.1$, and $\overline{\sigma}_1 = 0.045\ 5$. Keep the shape of metal foam unchanged. The force increases with the increase of the number of the metal layers in FML for the given deflection in Fig. 5(a). In Fig. 5(b), the maximum deflection of the rectangular foam-filled FML tube decreases with the increase of the number of the metal layers in FML for the given impact energy.

Figure 7 shows the effect of foam strength on the force versus deflection curve and maximum deflection curve with initial impact energy of foam-filled FML tubes, in which $G^* = 100$, $q = 2.1$,

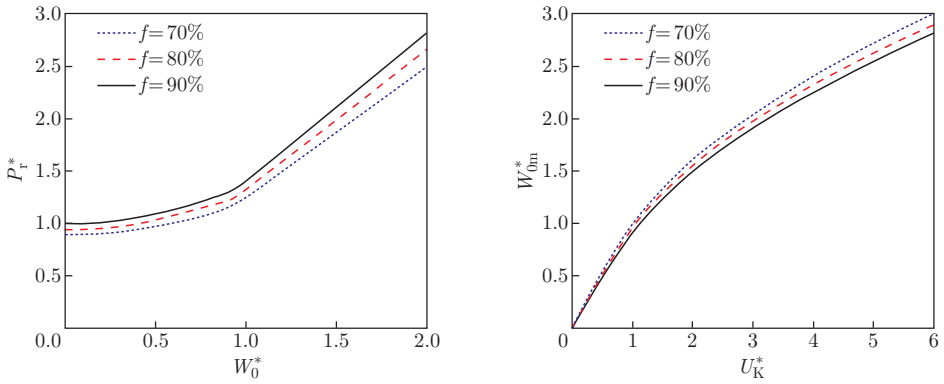

(a) Force-deflection curve (b) Maximum deflection curve with initial impact energy

Fig. 5 Effect of metal volume fraction in FML on low-velocity impact of foam-filled FML tubes (color online)

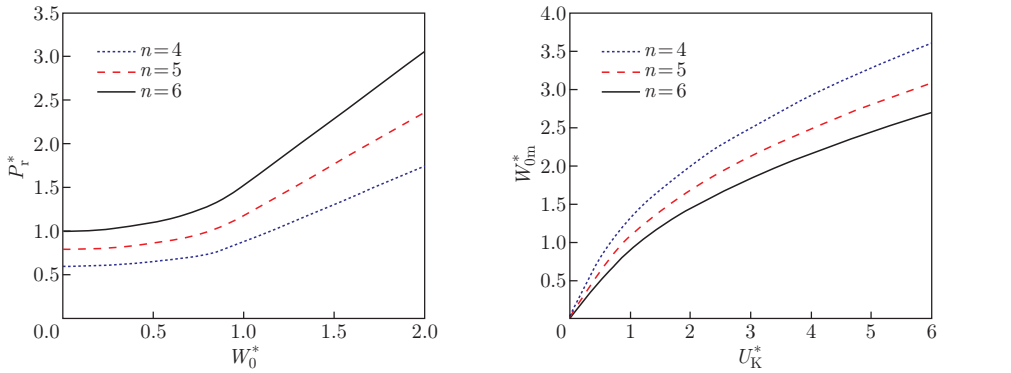

(a) Force-deflection curve (b) Maximum deflection curve with initial impact energy

Fig. 6 Effect of number of metal layers on low-velocity impact of foam-filled FML tubes (color online)

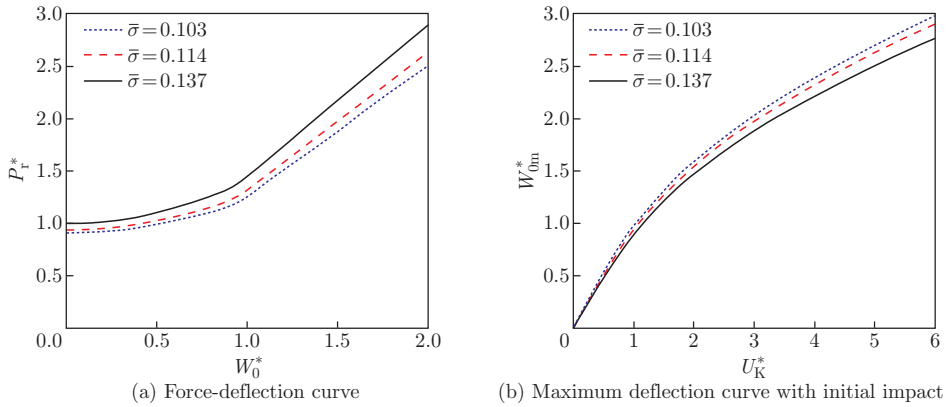

(a) Force-deflection curve (b) Maximum deflection curve with initial impact energy

Fig. 7 Effect of foam strength on low-velocity impact of foam-filled FML tubes (color online)

$n = 2$, $f = 83.3\%$, $\overline{h}_{\mathrm{f}} = 0.01$, and $\overline{\sigma}_1 = 0.045\,5$. The bigger the foam strength is, the more the increase in load-carrying capacity of the foam-filled FML tube is in Fig. 7(a). In Fig. 7(b), the maximum deflection of the rectangular foam-filled FML tube decreases with the increase of the

foam strength for the given impact energy.

6 Conclusions

In this paper, the low-velocity impact of a clamped rectangular foam-filled FML tube is analytically and numerically studied. According to rigid-plastic material approximation with modifications, simple analytical solutions for the force-deflection and initial impact energy-maximum deflection relations of rectangular foam-filled FML tubes at mid-span subject to low-velocity impact are presented. The analytical model captures numerical results reasonably, which proves the accuracy of the analytical and numerical results each other. The force increases with increase in metal volume fraction of FML, the number of the metal layers in FML, and the foam strength for the given deflection. The maximum deflection decreases with the increase of metal volume fraction of FML, the number of the metal layers in FMLs and the foam strength for the given initial impact energy. It is shown that the number of the metal layers in FMLs has a significant effect on the force-deflection and initial impact energy-maximum deflection relations.

References

[1] XU, Y. M., LI, H. G., YANG, Y. F., HU, Y. B., and TAO, J. Determination of residual stresses in Ti/CFRP laminates after preparation using multiple methods. *Composite Structures*, **210**, 715–723 (2019)

[2] LI, H. G., XU, Y. W., HUA, X. G., LIU, C., and TAO, J. Bending failure mechanism and flexural properties of GLARE laminates with different stacking sequences. *Composite Structures*, **187**, 354–363 (2018)

[3] AMIRI, A., MOHAMMADIMEHR, M., and ANVARI, M. Stress and buckling analysis of a thick-walled micro sandwich panel with a flexible foam core and carbon nanotube reinforced composite (CNTRC) face sheets. *Applied Mathematics and Mechanics* (*English Edition*), **41**(7), 1027–1038 (2020) https://doi.org/10.1007/s10483-020-2627-7

[4] ZHOU, H. Y., JIA, K. C., WANG, X. J., XIONG, M. X., and WANG, Y. H. Experimental and numerical investigation of low velocity impact response of foam concrete filled auxetic honeycombs. *Thin-Walled Structures*, **154**, 106898 (2020)

[5] JING, L., LIU, K., SU, X. Y., and GUO, X. Experimental and numerical study of square sandwich panels with layered-gradient foam cores to air-blast loading. *Thin-Walled Structures*, **161**, 107445 (2021)

[6] LU, Z. X., HUANG, J. X., and YUAN, Z. S. Effects of microstructure on uniaxial strength asymmetry of open-cell foams. *Applied Mathematics and Mechanics* (*English Edition*), **36**(1), 37–46 (2015) https://doi.org/10.1007/s10483-015-1893-9

[7] XIANG, X. M., ZOU, S. M., HA, N. S., LU, G. X., and KONG, I. Energy absorption of bio-inspired multi-layered graded foam-filled structures under axial crushing. *Composites Part B*: *Engineering*, **198**, 108216 (2020)

[8] ZHANG, J. X., QIN, Q. H., XIANG, C. P., and WANG, T. J. Plastic analysis of multilayer sandwich beams with metal foam cores. *Acta Mechanica*, **227**(9), 2477–2491 (2016)

[9] ZHANG, J., QIN, Q., AI, W., WANG, Z., and WANG, T. J. Indentation of metal foam core sandwich beams: experimental and theoretical investigations. *Experimental Mechanics*, **56**(5), 771–784 (2016)

[10] AFHBY, M. F., EVANS, A. G., FLECK, N. A., GIBSON, L. J., HUTCHINSON, J. W., and WADLEY, H. N. G. *Metal Foams*: *a Design Guide*, Butterworth-Heinemann, Boston, MA (2000)

[11] HALL, I. W., GUDEN, M., and CLAAR, T. D. Transverse and longitudinal crushing of aluminum-foam filled tubes. *Scripta Materialia*, **46**, 513–518 (2002)

[12] NIKNEJAD, A., ELAHI, S. A., and LIAGHAT, G. H. Experimental investigation on the lateral compression in the foam-filled circular tubes. *Materials & Design*, **36**, 24–34 (2012)

[13] NIKNEJAD, A., ASSAEE, H., ELAHI, S. A., and GOLRIZ, A. Flattening process of empty and polyurethane foam-filled E-glass/vinylester composite tubes—an experimental study. *Composite Structures*, **100**, 479–492 (2013)

[14] FANG, J. G., GAO, Y. K., SUN, G. Y., ZHANG, Y. T., and LI, Q. Parametric analysis and multiobjective optimization for functionally graded foam-filled thin-wall tube under lateral impact. *Computational Materials Science*, **90**, 265–275 (2014)

[15] NIKNEJAD, A. and RAHMANI, D. M. Experimental and theoretical study of the lateral compression process on the empty and foam-filled hexagonal columns. *Materials & Design*, **53**, 250–261 (2014)

[16] YAN, L. B., CHOUW, N., and JAYARAMAN, K. Lateral crushing of empty and polyurethane-foam filled natural flax fabric reinforced epoxy composite tubes. *Composites Part B: Engineering*, **63**, 15–26 (2014)

[17] ELAHI, S. A., ROUZEGAR, J., NIKNEJAD, A., and ASSAEE, H. Theoretical study of absorbed energy by empty and foam-filled composite tubes under lateral compression. *Thin-Walled Structures*, **114**, 1–10 (2017)

[18] SU, M. M., WANG, H., and HAO, H. Axial and radial compressive properties of alumina-aluminum matrix syntactic foam filled thin-walled tubes. *Composite Structures*, **226**, 111197 (2019)

[19] ZHANG, B. Y., WANG, L., ZHANG, J., JIANG, Y. X., WANG, W., and WU, G. H. Deformation and energy absorption properties of cenosphere/aluminum syntactic foam-filled circular tubes under lateral quasi-static compression. *International Journal of Mechanical Sciences*, **192**, 106126 (2021)

[20] ZHU, G. H., ZHAO, Z. H., HU, P., LUO, G., ZHAO, X., and YU, Q. On energy-absorbing mechanisms and structural crashworthiness of laterally crushed thin-walled structures filled with aluminum foam and CFRP skeleton. *Thin-Walled Structures*, **160**, 107390 (2021)

[21] AN, X. Z., GAO, Y. K., FANG, J. G., SUN, G. Y., and LI, Q. Crashworthiness design for foam-filled thin-walled structures with functionally lateral graded thickness sheets. *Thin-Walled Structures*, **91**, 63–71 (2015)

[22] SHIRAVAND, A. and ASGARI, M. Hybrid metal-composite conical tubes for energy absorption; theoretical development and numerical simulation. *Thin-Walled Structures*, **145**, 106442 (2019)

[23] MAMSOR, M. A., AHMAD, Z., and ABDULLAH, M. R. Experimental studies on the impact characteristics of seamless fibre metal laminate (FML) tubes. *Materials Today: Proceedings*, **39**, 1077–1081 (2021)

[24] JONES, N. Note on the impact behaviour of fibre-metal laminates. *International Journal of Impact Engineering*, **108**, 147–152 (2017)

[25] ZHANG, J. X., QIN, Q. H., YANG, Y., YU, X. H., XIE, S. J., and WANG, T. J. Dynamic response of foam-filled rectangular tubes subjected to low-velocity impact. *International Journal of Applied Electromagnetics and Mechanics*, **59**(4), 1441–1449 (2019)

[26] TAGARIELLI, V. L., FLECK, N. A., and DESHPANDE, V. S. Collapse of clamped and simply supported composite sandwich beams in three-point bending. *Composites Part B: Engineering*, **35**(6-8), 523–534 (2004)

[27] DESHPANDE, V. S. and FLECK, N. A. Isotropic constitutive models for metallic foams. *Journal of the Mechanics and Physics of Solids*, **48**(6-7), 1253–1283 (2000)